20

Measurement of the refractive index of biological tissues of the head using OCT and a multi-wavelength refractometer

© A.S. Shanshool¹, E.N. Lazareva^{1,3}¶, Yu.I. Surkov^{1,2}, I.A. Serebryakova^{1,2}, D.K. Tuchina^{1,2,3}, E.A. Genina^{1,3}, V.V. Tuchin^{1,2,3,4}

Received November 19, 2024 Revised November 29, 2024 Accepted April 07, 2025

Research and development in the field of laser biomedical diagnostics and therapy determine the interest in quantitative assessment of the optical properties of biological tissues, in particular the phase and group refractive index (RI). Knowledge of the optical dispersion dependencies of head tissues in a wide spectral range is necessary for the development of non-invasive methods for the diagnosis and treatment of brain diseases. In this regard, in this work, RI measurements were performed for rat head tissue samples (scalp, skull bone, dura mater, gray and white matter of the brain) *ex vivo* in the visible/near IR spectral range using optical coherence tomography (OCT) and a multi-wave Abbe refractometer for a number of laser wavelengths: 480, 486, 546, 589, 644, 656, 680, 800, 930, 1100, 1300 and 1550 nm. The phase RI values measured using a refractometer and determined from dispersion measurements and group RI at a central wavelength of 930 nm of an OCT system with a band of 100 nm were compared. The obtained RI values are in good agreement with known literature data.

Keywords: refractive index, optical coherence tomography, Abbe multi-wave refractometer, head biological tissues, dispersion formulas.

DOI: 10.61011/EOS.2025.05.61655.7028-24

1. Introduction

The refractive index (RI) of a biological tissue is a key parameter for characterizing the interaction of light with such a medium. Knowledge of RI of biotissues plays an important role in many biomedical applications. Malignant biological tissues can be distinguished in optical diagnostics from healthy ones by measuring and comparing their RI [1-3]. Optical coherence tomography (OCT) is a promising technology for measuring RI of layered highly scattering media, including biological tissues in vivo [4-11]. OCT is an interference imaging method that allows noninvasively obtaining optical cross-sectional images of samples, despite their strong scattering. Two- or threedimensional images of the sample can be reconstructed from numerous neighboring scans deep into the object — the socalled A-scans. OCT is widely used for imaging in a variety of biomedical studies [4–11].

There are several known methods that are successfully used to measure RI in biological tissues. One of the methods such as the Abbe method is based on the use of a prism of total internal reflection to determine the critical angle at which the RI of the medium is determined. A direct contact of the sample with the prism is required in this method, therefore, only the RI of a small layer in contact with the prism is measured [12–14]. Wang

et al. [2] used phase contrast microscopy to quantify the spatial variations of RI of tissues. Choi et al. [15] proposed a method for quantitative three-dimensional (3D) mapping of RI in living cells and tissues using a phase-shifting laser interferometric microscope based on a Mach-Zehnder interferometer and multi-angle scanning. This method requires complex algorithms for three-dimensional reconstruction and can only work for very thin tissue sections. Oliveira et al. [16] used the method of total internal reflection with an optical prism and lasers with different wavelengths to measure RI. Dirckx et al. [{]17 developed a method based on the use of a confocal microscope to measure the optical thickness of a sample, determined by its RI and geometric thickness, similar to OCT measurements.

The successful application of optical diagnostic and therapeutic methods in many cases requires reliable knowledge of the properties of biological tissues at many wavelengths, which is important for understanding the specifics of the dispersion of the medium during light propagation, predicting refractive characteristics, and analyzing diffraction and interference phenomena in tissues [18–25]. Unfortunately, there is a lack of sufficiently complete information in the known literature on the RI of many biological tissues, including head tissues. Most of the presented results [1–35] was either obtained for single wavelengths or averaged over a wide range of wavelengths. The lack of data is largely

¹ Saratov National Research State University n/a N.G. Chernyshevsky, Saratov, Russia

² Saratov National Research State University n/a N.G. Chernyshevsky, Saratov, Russia

³ Laboratory of Laser Molecular Imaging and Machine Learning, National Research Tomsk State University, Tomsk, Russia

⁴ Laboratory of Problems of Laser Diagnostics of Technical and Living Systems, Institute of Problems of Precision Mechanics and Control Systems, Saratov Scientific Center of the Russian Academy of Sciences, Saratov, Russia

[¶] e-mail: lazarevaen@list.ru

Table 1. Thickness of the studied *ex vivo* samples

Fabric samples	Thickness, mm
Scalp skin	0.58 ± 0.17
Skull bone	0.61 ± 0.19
DM	0.50 ± 0.15
Gray matter	0.49 ± 0.18
White matter	0.51 ± 0.19

explained by the difficulty of directly measuring the RI of dense highly diffuse biological tissues. Since it is necessary to know exactly the phase RI in order to calculate the absorption and scattering of biological tissues and simulate light propagation, the task of estimating it based on the measurement of group RI seems relevant.

Biological animal tissues are in many ways identical to human tissues in their structure and optical properties, therefore, many optical diagnostic and treatment methods are tested on laboratory animals, which makes it necessary to know the optical characteristics of healthy animal tissues, in particular the dispersion dependencies of RI. This paper presents experimental studies of group RI of laboratory rat head tissues, including scalp skin, skull bone, dura mater, gray and white matter of the brain using OCT (930 nm) and phase RI of gray matter of the brain using an Abbe multiwave refractometer with the results presented in the form of Sellmeier dispersion equations. In addition to obtaining new data for RI of head tissues in the visible and infrared regions of the spectrum, the purpose of this study is also to demonstrate, using the example of the gray matter of the brain, the possibility of restoring the value of phase RI from OCT measurements of group RI at a wavelength of 930 nm using the dispersion dependence near this wavelength, measured using a multiwave refractometer. The experimental data obtained for RI are compared with known literature data and with each other using the relationship between phase and group RI.

2. Methods and materials

2.1. Sample preparation

The studied samples of biological tissues were obtained from the vivarium of the Collective Use Center of the Saratov State Medical University named after V. I. Razumovsky after decapitation of healthy white Wistar rats. The animals were kept in standard vivarium conditions, all animal studies were performed in accordance with the International Rules for Biomedical Research using Animals [36] and approved by the Committee for the Care and Use of Laboratory Animals of Saratov National Research State University (Minutes 7, 02.07.2018).

For the *ex vivo* study, tissue samples (skin, skull bone, dura mater (DM), gray and white matter of the brain) were taken manually using a special scalpel (Fig. 1).

The skin areas were pre-shaved before excision. Skin samples were prepared from the scalps by removing the fat/muscle layer from the back of the scalp. 3 samples of each type of tissue were prepared for the study. The samples were immersed in saline solution for $10\,\mathrm{min}$ prior to the measurements to restore the physiological level of hydration. After that, the test samples were fixed on slides. The thickness of *ex vivo* samples was measured with an electronic micrometer with an accuracy of $\pm 1\,\mu\mathrm{m}$ at five different points and averaged over each sample (Table 1).

2.2. Experimental setups

Group RI measurements were performed for all samples of biological tissues using the OCM0930SR 022 spectral OCT system (Thorlabs, USA) operating at a central wavelength of 930 nm with a full spectrum width of a superluminescent diode at half height (FWHM) equal to 100 nm, with an axial resolution of 6.2, μ m in air and 4.4 μ m in fabric, maximum optical depth of 2.6 mm, axial scanning frequency of 1.2 kHz, transverse resolution of 8 μ m and sensitivity of 107 dB (Fig. 2, a).

Phase RI measurements were carried out at individual wavelengths using an Abbe DR-M2/1550 multiwave refractometer (Atago, Japan) (Fig. 2, b). Interference filters 480 ± 2 , 486 ± 2 , 546 ± 2 , 589 ± 2 , 644 ± 2 , 656 ± 2 , 680 ± 5 , 800 ± 8 , 930 ± 6 , 1100 ± 26 , 1300 ± 25 , 1550 ± 25 nm and a circulation thermostat were used for the study to maintain a constant temperature of the main measuring prism and sample (+22 °C). The refractometer was calibrated by measuring the RI of distilled water at a wavelength of 589 nm at the beginning of each measurement series. The average measurement error of RI was 0.0002.

3. Measurement results

3.1. OCT measurements

3 rats were used in ex vivo measurements, 3 samples of each type of tissue were prepared, a total of 15 samples of rat head tissues (skin, DM, skull bone, gray and white matter). The samples had a size of approximately 15×20 mm, and they were placed on slides for micropreparations SP-7101 (LLC "MiniLab", Russia) made of transparent, colorless silicate glass. The thickness of the glasses is approximately 1 mm. The fabrics on the slides were not fixed in a special way to avoid affecting their optical properties. The sample was placed in the OCT system in such a way that, when scanning along the surface of the sample, both the sample and the area in which the sample is missing could be observed. The RI of the fabric is determined by the displacement of the image of the upper surface of the slide under the sample [8,11,20,37-39]. The distance between the images of two points located on the same vertical scan line (A-scan) in the OCT image is equal to the optical path length between these two points (l),

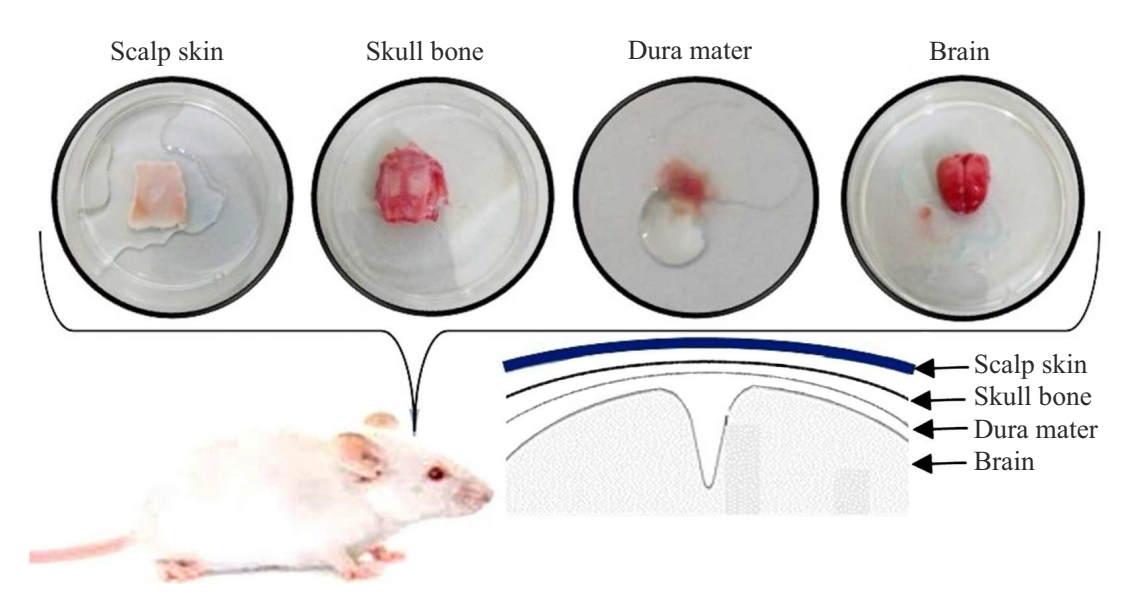


Figure 1. Rat head tissue samples.

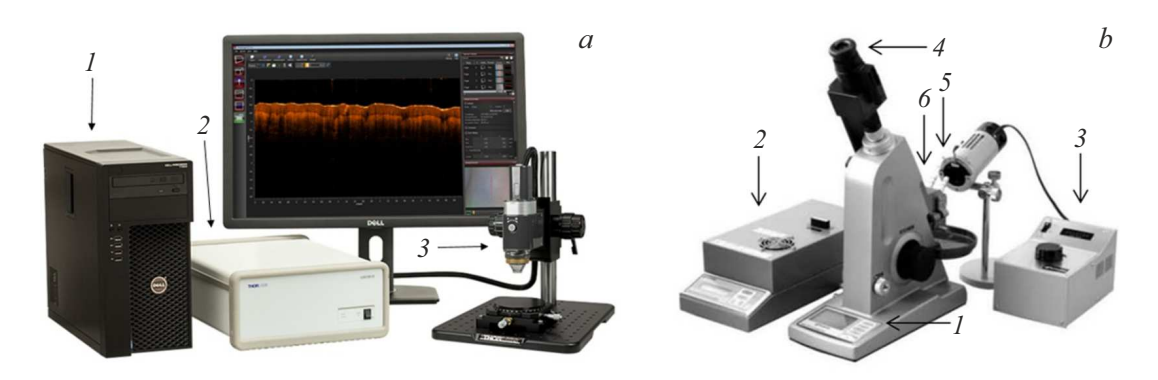


Figure 2. Experimental setups. (a) OCT system (930 nm): I — computer with software, 2 — OCT base unit with light source based on superluminescent diode, 3 — OCT probe. (b) Abbe Multiwave refractometer DR-M2/1550 (Atago, Japan): I — main unit with Abbe prism, 2 — power supply, 3 — broadband light source, 4 — visualizer for near-IR measurements, 5 — interference filter, 6 — sample.

determined through the average group RI of the medium on the path between these points (n_g) using the equation

$$l = n_{\rm g} d_{\rm s},\tag{1}$$

where d_s is the geometric distance between two points, measured between a line drawn through the upper point of the sample parallel to the substrate on which the sample lies and a line coinciding with the image of the upper part of the substrate in air (the middle line in the OCT image, as illustrated in Fig. 3).

In general, the sample can be not only in the air, but also surrounded by saline solution or immersion liquid, therefore, we denote the average group RI of the sample on this scan line as $n_{\rm g1}$. Then the optical path length through the sample on this scan line (two vertical arrows for $d_{\rm s}$ and $\Delta_{\rm R}$ in Fig. 3) will be defined as $l_{\rm s}=n_{\rm g1}d_{\rm s}$, where $d_{\rm s}$ —geometric length of the path through the sample. In the absence of a sample of the same geometric path length $d_{\rm s}$

, the optical path length $n_{\rm g0}d_{\rm s}$ would correspond, where $n_{\rm g0}$ is the group refractive index of the medium surrounding the sample (saline solution, immersion liquid, or air). The displacement of the image point of the upper surface of the slide in the presence of a sample relative to its position in the absence of a sample in the OCT image (arrow $\Delta_{\rm R}$ in Fig. 3) can be expressed as

$$\Delta_{\rm R} = l_{\rm s} - n_{\rm g0} d_{\rm s} = l_{\rm s} - n_{\rm g0} \frac{l_{\rm s}}{n_{\rm g1}}.$$
 (2)

Having determined l_s and Δ_R from the OCT image, it is possible to calculate the desired refractive index n_{g1} using the formula

$$n_{\rm g1} = \frac{n_{\rm g0}l_{\rm s}}{l_{\rm s} - \Delta_{\rm R}}.\tag{3}$$

The average group RI of the sample n_g was determined by averaging the values n_{g1} obtained for 3–5 averaged lines for A-scanning. The group RI of the tissue samples

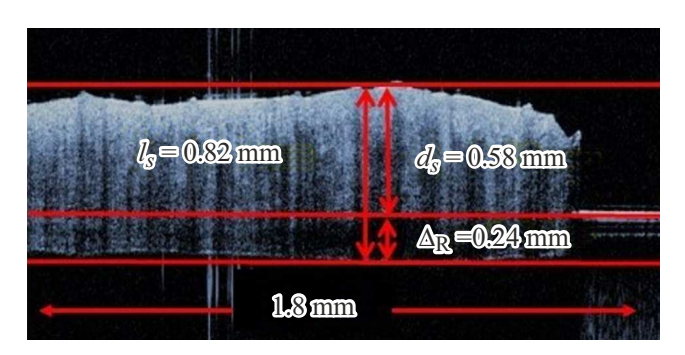


Figure 3. OCT-B-scan, recorded along the surface of the tissue sample and beyond its limits, where there is only air with RI close to 1, so the reflection from the upper part of the substrate on which the sample lies is clearly visible on the right, and its image is raised by an amount of Δ_R compared to the back border of the sample image (on the left).

Table 2. Experimental values of the group RI n_g of rat head tissues (SD — standard deviation) in the spectral range of $930 \pm 50 \text{ nm}$

Tissue	Average	Standard deviation
Scalp skin	1.429	0.006
Skull bone	1.510	0.016
DM	1.424	0.020
Gray matter	1.368	0.007
White matter	1.379	0.007

and environment was also calculated from the dispersion characteristics for the phase refractive index measured using an Abbe multiwave refractometer using the following general ratio [40]:

$$n_{\mathbf{g}}(\lambda_0) = n_{\mathbf{p}}(\lambda_0) - \lambda_0 \frac{dn_{\mathbf{p}}}{d\lambda}|_{\lambda = \lambda_0}, \tag{4}$$

where n_p is the phase RI of the medium, n_g is the group RI of the medium, λ_0 is the central wavelength in vacuum.

The group RI of saline solution during data processing was assumed to be approximately equal to the group RI of water. To calculate the group RI of water, data on the spectral dependence of the phase refractive index from Ref. [41] were used, which gave the value $n_{\rm g}=1.3416$ for $\lambda_0=930\,{\rm nm}$, which coincided well with the tabular value for water $n_{\rm g}=1.3420$ at a wavelength of 1014 nm [42]. To calculate the RI of the samples, it was assumed that for air $n_{\rm g0}~(930\,{\rm nm})=1$, and for saline solution $n_{\rm g0}~(930\,{\rm nm})=1.3416$.

30 A-scans were recorded to reduce speckle noise, which were averaged into one scan (time averaging). Two-dimensional OCT tomograms for *ex vivo* rat head tissue samples (scalp skin, skull bone, DM, gray matter, white matter) are shown in Fig.4, where the displacement of the image of the upper surface of the slide is clearly visible.

The OCT images clearly show differences in the structure of the cross-sectional images of the head tissue sections (Fig. 4, a, b) and the brain (Fig. 4, a, e). at the same time, the white matter of the brain (Fig. 4, e) has a higher intensity of the reflected signal sample/air than the sample of the gray matter of the brain (Fig. 4, e), which indicates a higher refractive index of the diffusers in a white matter medium. Indeed, the average group RI of white matter was 1.379, and for gray matter it was slightly less — 1.368. The difference between RI in each anatomical region may be related to different cell types, their density, and differences in the volume fractions of extracellular and intracellular matter in their structures.

Table 2 shows the data of measurement of the group RI of rat head tissues by the OCT method.

3.2. RI measurement using an Abbe refractometer

When measuring RI using an Abbe refractometer (Fig. 2, b), the wavelength of the light source is determined by the choice of an interference filter tuned to a specific The available interference filters allowed measurements to be carried out at the following central wavelengths in the band determined by the bandwidth of the filters at the FWHM level: $480(\pm 2)$, $486(\pm 2)$, $546(\pm 2)$, $589(\pm 2)$, $644(\pm 2)$, $656(\pm 2)$, $680(\pm 5)$, $800(\pm 8)$, $930(\pm 6)$, $1100(\pm 26)$, $1300(\pm 25)$ and $1550(\pm 25)$ nm. Many of these wavelengths are used in laser light sources. Since filters have a certain bandwidth, the refractometer measures the group RI $n_g(\lambda_0)$. To determine the value of the phase RI $n_{\rm p}(\lambda_0)$ at a given wavelength λ_0 , the ratio (4) was used, in which the dispersion $\frac{dn_p}{d\lambda}$ was approximated using the known dispersion RI of water [41]. Further, to approximate the dispersion dependence of the RI of the samples in the range of 480-1550 nm, the obtained values of the phase RI for each central wavelength $n_p(\lambda_0)$ and the Sellmeier formula were used

$$n_{\rm p}^2(\lambda) = 1 + \frac{A_1 \lambda^2}{\lambda^2 - B_1} + \frac{A_2 \lambda^2}{\lambda^2 - B_2},$$
 (5)

where A_1 , A_2 , B_1 and B_2 are empirical constants. The Sellmeier formula gives good agreement when describing the dispersion dependence of RI of multicomponent systems near the absorption bands of the studied medium [43–59]. Mathematical calculations were performed in the Origin ProLab software package (OriginLab Corp., USA).

The results of RI measurements on an Atago refractometer for distilled water (control) and gray matter of the rat brain at 12 wavelengths of the spectral range of 480–1550 nm at room temperature and the calculated values of the phase RI and their interpolation for 3 samples of each tissue type are presented in Table. 3.

Fig. 5 shows the dispersion curves for rat brain gray matter and distilled water, measured on an Abbe refractometer and calculated from these measurements the values of the phase RI $n_p(\lambda_0)$. The symbols represent

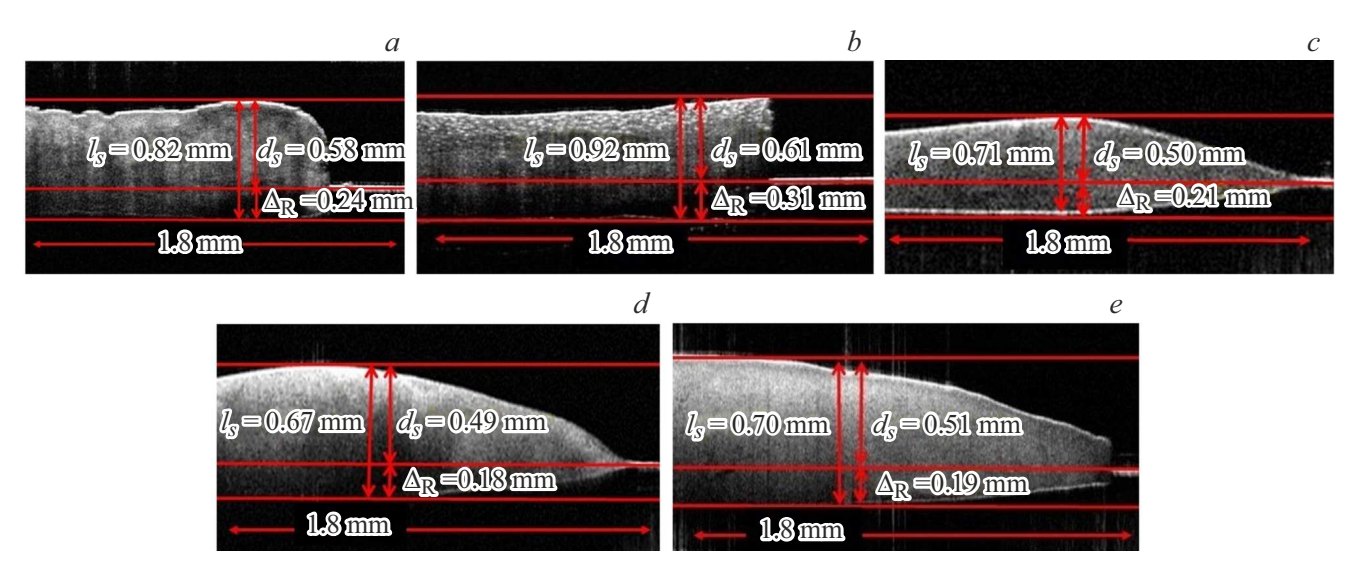


Figure 4. OCT-images of rat head tissue samples: scalp skin (a), skull bone (b), DM (c), gray matter of the brain (d) and white matter of the brain (e).

Table 3. The values of RI (average \pm standard deviation) of distilled water and gray matter of rat brain at room temperature of 22 °C, measured using Atago refractometer with interference filters and calculated from these measurements for the phase RI $n_p(\lambda_0)$

λ , nm	Refractive index Abbe Refractometer		Refractive index $n_{ m p}(\lambda_0)$		
•					
	Water (control)	Gray matter	Water (control)	Gray matter	
480	1.3366 ± 0.0049	1.3691 ± 0.0059	1.3371 ± 0.0061	1.3711 ± 0.0056	
486	1.3358 ± 0.0044	1.3689 ± 0.0075	1.3360 ± 0.0028	1.3696 ± 0.0049	
546	1.3342 ± 0.0042	1.3661 ± 0.0067	1.3344 ± 0.0063	1.3663 ± 0.0047	
589	1.3329 ± 0.0019	1.3645 ± 0.0066	1.3331 ± 0.0051	1.3652 ± 0.0036	
644	1.3313 ± 0.0027	1.3628 ± 0.0065	1.3320 ± 0.0046	1.3631 ± 0.0047	
656	1.3303 ± 0.0041	1.3621 ± 0.0065	1.3310 ± 0.0042	1.3628 ± 0.0057	
680	1.3299 ± 0.0019	1.3611 ± 0.0065	1.3306 ± 0.0029	1.3619 ± 0.0061	
800	1.3283 ± 0.0029	1.3591 ± 0.0062	1.3289 ± 0.0041	1.3596 ± 0.0066	
930	1.3257 ± 0.0028	1.3572 ± 0.0062	1.3267 ± 0.0037	1.3579 ± 0.0058	
1100	1.3225 ± 0.0036	1.3537 ± 0.0065	1.3233 ± 0.0029	1.3541 ± 0.0049	
1300	1.3179 ± 0.0061	1.3490 ± 0.0062	1.3181 ± 0.0027	1.3496 ± 0.0043	
1550	1.3135 ± 0.0047	1.3452 ± 0.0059	1.3139 ± 0.0041	1.3466 ± 0.0057	

Table 4. Decomposition coefficients of the refractive index of rat brain gray matter and distilled water according to the Sellmeier formula in the region of 480–1550 nm

Coefficients Sellmeier	A_1	A_2	B_1, nm^{-2}	B_2 , 10^{10} nm ⁻²	R^2
Distilled water	0.76671	718.67	6876.16	3.8869	0.996
Gray matter	0.84646	688.26	8392.12	4.064	0.996

experimental data from Table 4, and the lines correspond to an approximation of these data according to the Sellmeier formula (equation(5)), the parameters of which are given in Table 4.

As follows from Table 4, for rat brain gray matter and distilled water, the measured RI values correspond well to the Sellmeier formula with a correlation coefficient R^2 equal to or better than 0.987 and 0.991, respectively.

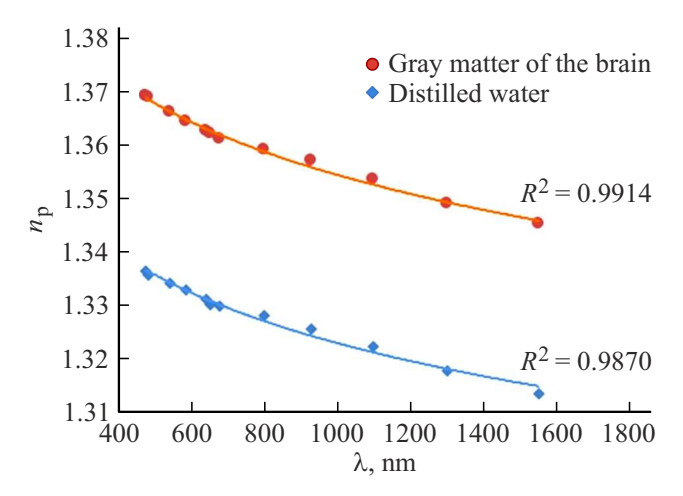


Figure 5. Dispersion relations for phase RI $n_p(\lambda_0)$ of rat brain gray matter and distilled water, calculated using measurements on an Atago refractometer.

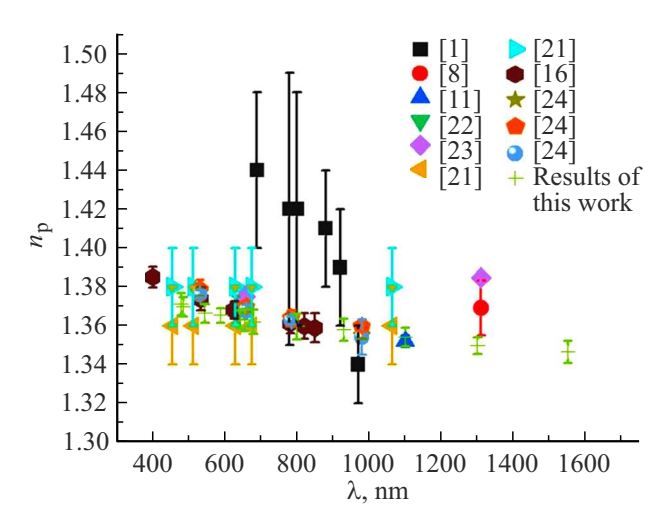


Figure 6. Comparison of the values of the phase RI for the gray matter of the rat brain obtained in this paper with the results of other studies (Table 3 and 6).

Table 5. Values of the group RI $(n_{\rm g}^{\rm OCT})$ measured using OCT and the phase RI calculated from these measurements $(n_{\rm p}^{\rm OCT})$, as well as the phase RI $(n_{\rm p}^{\rm Abbe})$ obtained from measurements on Abbe refractometer, for measuring the gray matter of the rat brain

λnm	$n_{ m g}^{ m OCT}$	$n_{ m p}^{ m OCT}$	$n_{ m p}^{ m Abbe}$
930	1.368 ± 0.007	1.351 ± 0.006	1.3572 ± 0.0062

3.3. Discussion of the results

The results obtained for measurements of the group RI using OCT and the dispersion of the phase RI using a multiwave refractometer make it possible to calculate the value of the phase RI refraction at a wavelength of 930 nm from the data for OCT and compare them with the data

of measurements of the phase RI on a refractometer using the example of the gray matter of the rat brain. These data are presented in Table 5, which shows the group RI $(n_{\rm g}^{\rm OCT})$ and the phase RI $(n_{\rm p}^{\rm OCT})$ calculated using the formula (4) from OCT measurements based on the dispersion curve obtained using refractometric measurements, as well as the phase RI $(n_{\rm p}^{\rm Abbe})$ at a wavelength of 930 nm, determined using a refractometer taking into account the finite width of the corresponding interference filter. It is clearly seen that the measured and calculated values of the phase RI differ slightly from each other, which is within the experimental measurement error of OCT and sample variability — the difference is 0.006.

The relevant literature data are provided in Table 6 for comparing the data obtained in this paper for RI of head tissues.

The summary data provided in Table 3 and 6 make it possible to compare the experimental data obtained in this work with the literature data. Thus, according to the results of study in Ref. [8], where OCT measurements were performed at an average wavelength of 1310 nm for sections of gray and white matter of the rat brain, $n_{\rm g} = 1.369 \pm 0.014$ and 1.407 ± 0.015 , which coincides well with the data of this study $n_{\rm g}=1.368\pm0.007$ and 1.379 ± 0.007 , taking into account the differences in central wavelengths. The values of the phase RI of the gray matter of the rat brain in our measurements (Table. 3), equal to $n_p = 1.3631 \pm 0.0047$ at a wavelength of 644 nm and $n_{\rm p}=1.3619\pm0.0061$ at a wavelength of 680 nm, correspond well to the values of the phase RI slice of the mouse brain measured at approximately the same wavelengths, $n_{\rm p} = 1.368 \pm 0.007$ for 633 nm [22] and $n_{\rm p} = 1.44 \pm 0.04$ for 690 nm [1]. The phase RI of the gray matter of the human brain at wavelengths of 456/514/630/675/1064 nm, equal to $n_p = 1.36 \pm 0.02$ [21], also fits well into the general data within the differences between human and animal brain RI. Different scientific groups have obtained very similar results for the study of gray matter in the rabbit brain: $n_p = 1.3736 \pm 0.0058$ at 534.6 nm [16] and $n_{\rm p} = 1.3761 \pm 0.0020$ at 532 nm [24].

For clarity, Figure 6 shows a comparison of the experimental data obtained in this work for the phase RI of the gray matter of the rat brain with the literature data from Table 6.

The experimental data obtained in this study for the values of the phase RI of the gray matter of the brain are in good agreement with the literature data for animals and humans, and the observed differences may most likely be related to different methods of measuring phase RI, with sample preparation and their physiological characteristics.

4. Conclusion

This paper presents the results of measurements of one of the most important optical parameters of biological media — RI of five types of rat head tissues (scalp skin,

Table 6. Comparison of the obtained results with the literature data

Tissue	Wave- length, nm	Refractive index	Measurement method, literature
Mouse brain	690 780 800 880 920 970	$\begin{aligned} 1.44 &\pm 0.04 \\ 1.42 &\pm 0.07 \\ 1.42 &\pm 0.06 \\ 1.41 &\pm 0.03 \\ 1.39 &\pm 0.03 \\ 1.34 &\pm 0.02 \end{aligned}$	Method of spatial modulation of diffuse reflection, n_p [1]
Mouse brain: slice $5 \mu m$, fixed	633	1.368 ± 0.007	Hilbert phase microscopy, n_p [22]
Cellular bodies cortical neurons mice in culture (2 individual cells)	658	1.3751 ± 0.0003 1.3847 ± 0.0003	Digital holographic microscopy, n_p [23]
Human brain: gray matter; white matter	456/514/630 /675/1064	$1.36 \pm 0.02 \\ 1.38 \pm 0.02$	Multiple laser reflection from thin tissue samples, n_p [21]
Rabbit's brain: gray matter; white matter	456/514/630 /675/1064	$\begin{array}{c} 1.36 \pm 0.02 \\ 1.36 \pm 0.02 \end{array}$	Multiple laser reflection from thin tissue samples, n_p [21]
Rabbit's brain: gray matter, ex vivo	401.4 534.6 626.6 782.1 820.8 850.0	$\begin{array}{c} 1.3850 \pm 0.0053 \\ 1.3736 \pm 0.0058 \\ 1.3680 \pm 0.0045 \\ 1.3611 \pm 0.0050 \\ 1.3597 \pm 0.0066 \\ 1.3589 \pm 0.0076 \end{array}$	Prismatic laser method, n_p [16]
Scalp skin rabbit, ex vivo	532 660 785 980	$\begin{aligned} 1.3769 &\pm 0.002 \\ 1.3691 &\pm 0.002 \\ 1.3631 &\pm 0.003 \\ 1.3551 &\pm 0.002 \end{aligned}$	Prismatic laser method, n_p [24]
Skull bone rabbit, ex vivo	532 660 785 980	$\begin{aligned} 1.3784 &\pm 0.005 \\ 1.3695 &\pm 0.001 \\ 1.3637 &\pm 0.004 \\ 1.3596 &\pm 0.002 \end{aligned}$	Prismatic laser method, n_p [24]
Rabbit's brain ex vivo	532 660 785 980	$\begin{array}{c} 1.3761 \pm 0.002 \\ 1.3676 \pm 0.003 \\ 1.3626 \pm 0.002 \\ 1.3541 \pm 0.009 \end{array}$	Prismatic laser method, n_p [24]
Rat's brain: gray matter, white matter	1310	$\begin{array}{c} 1.369 \pm 0.014 \\ 1.407 \pm 0.015 \end{array}$	OCT, FWHM 75 nm, $n_{\rm g}$ [8]
Rat's brain: gray matter	1100	1.3526 ± 0.0029	OCT, FWHM 200 nm, n_p taking into account variance [11]
Scalp skin Skull bone DM Gray matter White matter	930	$egin{array}{l} 1.429 \pm 0.006 \\ 1.510 \pm 0.016 \\ 1.424 \pm 0.020 \\ 1.368 \pm 0.007 \\ 1.379 \pm 0.007 \end{array}$	OCT, n_g , FWHM 100 nm, this study

skull bone, DM, gray and white matter of the brain) ex vivo OCT (at a wavelength of 930 nm in the band 100 nm) and for the gray matter of the rat brain using an Abbe multiwave refractometer (in the wavelength range from 480 to 1550 nm). The gray matter tissue of the brain showed a normal dispersion with a decrease in RI with an increase in wavelength. A comparison of the values of the phase RI for the gray matter of the rat brain, measured using an Abbe prism refractometer and calculated from the measurements of the group RI using OCT, taking into account the measured dispersion of RI near the central wavelength OCT 930 nm. It is clearly seen that the measured and calculated values of the phase RI differ slightly from each other, which is within the experimental measurement error of OCT and sample variability 0.006. The obtained values of RI are in good agreement with the known literature data. These results are of great practical value for the development and application of methods for modeling the propagation of optical radiation in head tissues to solve direct and inverse problems of optical biopsy and imaging, including selective immersion illumination of individual tissues to improve the quality and increase the depth of the images obtained.

Funding

The study was supported by the Russian Science Foundation grant No 23-14-00287.

Conflict of interest

The authors declare that they have no conflict of interest.

References

- [1] D. Abookasis, O. Meitav. In: Proc. SPIE 10864, Clinical and Translational Neurophotonics 2019, 108640R (2019).
- [2] Z. Wang, K. Tangella, A. Balla, G. Popescu. J. Biomed. Opt., 16 (11), 116017 (2011). DOI: 10.1117/1.3656732
- [3] E.N. Lazareva, V.V. Tuchin. J. Biomed. Opt., 23 (3), 1–9 (2018). DOI: 10.1117/1.JBO.23.3.035004
- [4] E. Osiac, S.I. Mitran, C.N. Manea, A. Cojocaru, G.C. Rosu, M. Osiac, D.N. Pirici, A.T. Bălşeanu, B. Cătălin. Microsc. Res. Tech., 84 (3), 422–431 (2021). DOI: 10.1002/jemt.23599
- [5] J.M. Lee, I. Han, K.H. Nam, D.H. Kim, S. Song, H. Park, H. Kim, M. Kim, J. Choi, J.I. Lee. J. Biophotonics, 14 (11), e202100143 (2021). DOI: 10.1002/jbio.202100143
- [6] J. Möller, A. Bartsch, M. Lenz, I. Tischoff, R. Krug, H. Welp, M.R. Hofmann, K. Schmieder, D. Miller. Int. J. Comput. Assist. Radiol. Surg., 16 (9), 1517–1526 (2021). DOI: 10.1007/s11548-021-02412-2
- [7] A.J. Fitzgerald, X. Tie, M.J. Hackmann, B. Cense, A.P. Gibson, V.P. Wallace. Biomed. Opt. Express, 11 (3), 1417–1431 (2020). DOI: 10.1364/BOE.378506
- [8] J. Sun, S.J. Lee, L. Wu, M. Sarntinoranont, H. Xie. Opt. Express, 20 (2), 1084–95 (2012). DOI: 10.1364/OE.20.001084
- [9] C.J. Liu, W. Ammon, R.J. Jones, J. Nolan, R. Wang, S. Chang, M.P. Frosch, A. Yendiki, D.A. Boas, C. Magnain, B. Fischl, H. Wang. Biomed. Opt. Express, 13 (1), 358–372 (2021).

- [10] G. Min, W.J. Choi, J.W. Kim, B.H. Lee. Opt. Express, 21 (24), 29955–67 (2013). DOI: 10.1364/OE.21.029955
- [11] J. Binding, J. Ben Arous, J.F. Léger, S. Gigan, C. Boccara, L. Bourdieu. Opt. Express, 19 (6), 4833–47 (2011). DOI: 10.1364/OE.19.004833
- [12] A.S. Shanshool, E.N. Lazareva, V.V. Tuchin. In: Proc. SPIE 12192, Optical Technologies for Biology and Medicine, 1219212 (2022). DOI: 10.1117/12.2634156
- [13] A. García-Valenzuela, H. Contreras-Tello. Opt. Lett., 38 (5), 775–7 (2013). DOI: 10.1364/OL.38.000775
- [14] X. Xu, R.K. Wang, J.B. Elder, V.V. Tuchin. Phys. Med. Biol., 48 (1), 1205–1221 (2003).
- [15] W. Choi, C. Fang-Yen, K. Badizadegan, S. Oh, N. Lue, R.R. Dasari, M.S. Feld. Nat. Methods, 4 (9), 717–9 (2007). DOI: 10.1038/nmeth1078
- [16] T.M. Gonçalves, I.S. Martins, H.F. Silva, V.V. Tuchin,
 L.M. Oliveira. Photochem., 1 (2021), 190–208 (2021).
 DOI: 10.3390/photochem1020011
- [17] J.J. Dirckx, L.C. Kuypers, W.F. Decraemer. J. Biomed. Opt., 10 (4), 44014 (2005). DOI: 10.1117/1.1993487
- [18] P. Sawosz, S. Wojtkiewicz, M. Kacprzak, W. Weigl, A. Borowska-Solonynko, P. Krajewski, A. Liebert. Biomed. Opt. Express, 7 (1), 5010–5020 (2016).
- [19] J. Yang, I.A. Chen, S. Chang, J. Tang, B. Lee, K. Kılıç, S. Sunil, H. Wang, D. Varadarajan, C. Magnain, S.C. Chen, I. Costantini, F. Pavone, B. Fischl, D.A. Boas. Neurophotonics, 7 (4), 045005 (2020).
- [20] M.E. Shvachkina, D.D. Yakovlev, E.N. Lazareva, A.B. Pravdin, D.A. Yakovlev. Opt. i spektr., 2 (127), 337–346 (2019) (in Russian).
- [21] W. Gottschalk. Ein Messverfahren zur Bestimmung der optischen Parameter biologischer Gewebe in vitro (Universität Karlsruhe, Karlsruhe, 1993).
- [22] N. Lue, J. Bewersdorf, M.D. Lessard, K. Badizadegan, R.R. Dasari, M.S. Feld, G. Popescu. Opt. Lett., 32 (24), 3522-3524 (2007).
- [23] B. Rappaz, P. Marquet, E. Cuche, Y. Emery, C. Depeursinge,P. Magistretti. Opt. Express, 13 (23), 9361–9373 (2005).
- [24] A.S. Shanshool, E.N. Lazareva, O. Hamdy, V.V. Tuchin. Materials, 15 (1), 5696 (2022). DOI: 10.3390/ma15165696
- [25] J. Stritzel, M. Rahlves, B. Roth. Opt. Lett., 40 (23), 5558-5561 (2015). DOI: 10.1364/OL.40.005558
- [26] T. Das, K. Bhattacharya. Appl. Opt., 56 (33), 9241–9246 (2017).
- [27] J. Wang, Z. Deng, X. Wang, Q. Ye, W. Zhou, J. Mei, C. Zhang, J. Tian. Biomed. Opt. Express, 6 (7), 2536–2541 (2015).
- [28] H. Ding, J.Q. Lu, W.A. Wooden, P.J. Kragel, X-H. Hu. Phys. Med. Biol., 51 (6), 1479–1489 (2006).
- [29] M. Matiatou, P. Giannios, S. Koutsoumpos, K.G. Toutouzas, G.C. Zografos, K. Moutzouris. Results in Physics, 22 (1), 103833 (2021).
- [30] A. Knuttel, S. Bonev, W. Knaak. J. Biomed. Opt., 9 (2), 265–273 (2004).
- [31] S. Kim, J. Na, M.J. Kim, B.H. Lee. Opt. Express, 16 (8), 5516 (2008).
- [32] D.F. Murphy, D.A. Flavin. Appl. Opt., **39** (1), 4607–4615 (2000).
- [33] T. Fukano, I. Yamaguchi. Appl. Opt., 38 (1), 4065–4073 (1999).
- [34] S.A. Alexandrov, A.V. Zvyagin, K.K.M.B.D. Silva, D.D. Sampson. Opt. Lett., 28, 117–119 (2003).

- [35] X. Wang, C. Zhang, L. Zhang, L. Wu, J. Tian. J. Biomed. Opt., 7, 628–632 (2002).
- [36] CIOMS&ICLAS, URL: https://iclas.org/cioms-and-iclas
- [37] W.V. Sorin, D.F. Gray. IEEE Photonics Technology Letters, 4 (1), 105–107 (1992).
- [38] M.S. Wróbel, A.P. Popov, A.V. Bykov, M. Kinnunen, M. Jędrzejewska-Szczerska, V.V. Tuchin. J. Biomed. Opt., 20 (4), 045004 (2015).
- [39] D.A. Zimnyakov, A.B. Pravdin, L.V. Kuznetsova, V.I. Kochubey, V.V. Tuchin, R.K. Wang, O.V. Ushakova. JOSA, 24 (3), 711–723 (2007).
- [40] M. Born, E. Wolf. Principles of optics: Electromagnetic theory of propagation, interference and diffraction of light, 6th ed. (Pergamon Press-Elsevier, Oxford, 2013).
- [41] M. Daimon, A. Masumura. Appl. Opt., 46 (18), 3811–3820 (2007). DOI: 10.1364/ao.46.003811
- [42] M.N. Polyanskiy. Scientific Data, 11 (94), (2024). DOI: 10.1038/s41597-023-02898-2
- [43] O. Zhernovaya, O. Sydoruk, V. Tuchin, A. Douplik. Phys. Med. Biol., 56 (13), 4013–4021 (2011). DOI: 10.1088/0031-9155/56/13/017
- [44] O. Sydoruk, O. Zhernovaya, V. Tuchin, A. Douplik. J. Biomed. Opt., 17 (11), 115002 (2012). DOI: 10.1117/1.JBO.17.11.115002
- [45] E.N. Lazareva, V.V. Tuchin. J. Biomed. Photon. Eng., 4 (1), 010503 (2018).
- [46] I.Y. Yanina, A.P. Popov, A.V. Bykov, I.V. Meglinski, V.V. Tuchin. J. Biomed. Opt., 23 (1), 016003 (2018). DOI: 10.1117/1.JBO.23.1.016003
- [47] A.N. Bashkatov, K.V. Berezin, K.N. Dvoretskiy, M.L. Chernavina, E.A. Genina, V.D. Genin, V.I. Kochubey, E.N. Lazareva, A.B. Pravdin, M.E. Shvachkina, P.A. Timoshina, D.K. Tuchina, D.D. Yakovlev, D.A. Yakovlev, I.Yu. Yanina, O.S. Zhernovaya, V.V. Tuchin. J. Biomed. Opt., 23 (9), 091416 (2018). DOI: 10.1117/1.JBO.23.9.091416
- [48] I. Carneiro, S. Carvalho, V. Silva, R. Henrique, L. Oliveira, V.V. Tuchin. J. Biomed. Opt., 23 (12), 121620 (2018). DOI: 10.1117/1.JBO.23.12.121620
- [49] G.J. Tearney, M.E. Brezinski, J.F. Southern, B.E. Bouma, M.R. Hee, J.G. Fujimoto. Opt. Lett., 20 (21), 2258–2260 (1995).
- [50] H. Fu, W. Gao, Z. Lin, Z. Zeng, W. Shi, J. Zhang. Photonics, MDPI, 10 (7), 841 (2023).
- [51] R. Khan, B. Gul, Sh. Khan, H. Nisar, I. Ahmad. Photodiagnosis and Photodynamic Therapy, 33 (1), 102192 (2021).
- [52] H. Maruyama, S. Inoue, T. Mitsuyama, M. Ohmi, M. Haruna. Appl. Opt., 41, 1315–1322 (2002).
- [53] M. Ohmi, H. Nishi, T. Konishi, Y. Yamada, M. Haruna. Meas. Sci. Technol., 15, 1531–1535 (2004).
- [54] A. Shirkavand, S. Farivar, E. Mohajerani, L. Ataie-Fashtami, M.H. Ghazimoradi. Lasers in Surgery and Medicine, 51 (8), 742–750 (2019). DOI: 10.1002/lsm.23095
- [55] C. Cairos, R. Oliva-García, G. Siverio, J. M. Trujillo-Sevilla, J. Manuel Rodríguez-Ramos, A. Acebes. Opt. Materials, 142, 114087 (2023).
- [56] L. Benatto, O. Mesquita, L.S. Roman, M. Koehler, R.B. Capaz, G. Candiotto. Computer Physics Commun., 298, 109100 (2024). DOI: 10.1016/j.cpc.2024.109100
- [57] E.N. Lazareva, L. Oliveira, I.Yu. Yanina, N.V. Chernomyrdin, G.R. Musina, D.K. Tuchina, A.N. Bashkatov, K.I. Zaytsev, V.V. Tuchin. Refractive index measurements of tissue and blood components and OCAs in a wide spectral range.

- In: Handbook of tissue optical clearing: New prospects in optical imaging, eds. V.V. Tuchin, D. Zhu, E.A. Genina (Taylor & Francis Group LLC, CRC Press, Boca Raton, FL, 2022).
- https://www.routledge.com/Handbook-of-Tissue-Optical-Clearing-New-Prospects-in-Optical-Imaging/Tuchin-Zhu-Genina/p/book/9780367895099
- [58] I.S. Martins, H.F. Silva, E.N. Lazareva, N.V. Chernomyrdin, K.I. Zaytsev, L.M. Oliveira, V.V. Tuchin. Biomed. Opt. Express, 14 (1), 249–298 (2023). DOI: 10.1364/BOE.479320
- [59] I.Yu. Yanina, E.N. Lazareva, V.V. Tuchin. Appl. Opt., 57 (17), 4839–4848 (2018). DOI: 10.1364/AO.57.004839

Translated by A.Akhtyamov